Viscosity of Two-Dimensional Suspensions

Junqi Ding, Heidi E. Warriner, and Joseph A. Zasadzinski*

Department of Chemical Engineering, University of California, Santa Barbara, California 93106-5080

(Received 12 July 2001; published 8 April 2002)

Over a range of conditions, lipid and surfactant monolayers exhibit coexistence of discrete solid domains in a continuous liquid. The surface shear viscosity, μ_s, of such monolayers collapses onto a single curve: $\mu_s/\mu_{so} = [1 - (A/A_c)]^{-1}$, in which μ_{so} is the viscosity of the liquid phase, A is the area fraction of the solid phase measured by fluorescence microscopy, and A_c is a critical solid phase fraction. This scaling relationship is directly analogous to that of three-dimensional dispersion of spheres in a solvent with long-range repulsive interactions, with area fraction replacing volume fraction.

DOI: 10.1103/PhysRevLett.88.168102 PACS numbers: 68.18.–g, 82.70.Uv, 83.80.–k

The morphology common to many technologically and biologically important monolayers [1–6] is a coexistence of discrete domains of long-range ordered "solid" phase dispersed in a continuous, disordered, liquid-expanded phase. We show that the viscous response of this monolayer morphology is the two-dimensional analog of three-dimensional suspensions of hard spheres in a solvent. In 3D suspensions, the effective viscosity scales as the number of particles in contact, divided by the short-time self-diffusivity at the sphere volume fraction of interest, ϕ [7]. For noninteracting hard spheres, as the volume fraction for random close packing ϕ_c is approached, the number of particles in contact diverges as $[1 - (\phi/\phi_c)]^{-1}$. The short time self-diffusivity vanishes as $[1 - (\phi/\phi_c)]$ because the particles are held in place by strong hydrodynamic lubrication forces. Thus, the reduced viscosity scales as $\mu/\mu_o = [1 - (\phi/\phi_c)]^{-2}$; μ is the steady shear viscosity of the dispersion and μ_o is the viscosity of the suspending fluid. However, if there are strong repulsive forces between the solid particles on a length scale large compared to the hydrodynamic lubrication forces, the short time self-diffusivity does not vanish. The viscosity still diverges as random close packing is approached, but as $\mu/\mu_o = [1 - (\phi/\phi_c)]^{-1}$. We have found that these scaling arguments are equally valid in two-dimensional monolayers at coexistence, with the area fraction of the solid phase replacing the volume fraction of hard spheres. Our observation that the surface viscosity scales as $\mu_s/\mu_{so} = [1 - (A/A_c)]^{-1}$ suggests that there is a strong repulsion between solid domains in the monolayer, which is consistent with the repulsive dipole-dipole interaction between solid phase domains in both charged and uncharged monolayers [1,2,8].

The monolayer shear viscosity is measured by determining the terminal velocity of a magnetic needle floated at the air/water interface in a Langmuir trough driven by the magnetic field gradient between two parallel electromagnetic coils [9,10]. Along the axis of the magnetic field gradient, there is a 3 cm wide channel made from two hydrophilic glass plates; the meniscus between the plates helps direct the magnetic needle encapsulated inside a 3 cm long, 1.9 mm diam hollow Teflon tube. Equal and oppositely directed current applied to two 61 cm diameter coils, separated by 61 cm, generates a uniform magnetic field gradient (varies $<1\%$). Two power supplies control current to the coils to adjust the magnitude of the magnetic field gradient (EXH 30-10, Electronic Measurements, Inc., NJ). The surface pressure is measured with a Wilhelmy plate (R&K, Germany). Above the channel, a video camera (Sony CCD-TR940) records the needle speed; the video signal is digitized (ST3155, Data Translations, Inc) to determine the needle velocity.

For a given applied force, F, the limiting velocity, v_1, is set by the sum of the viscous drag on the needle from the subphase and the monolayer [9,11,12]:

$$F = \left(\frac{\mu_s P_c}{L_c'} + \frac{\mu a_c}{L_c''}\right) v_1 . \tag{1}$$

P_c is the contact perimeter between the needle and the monolayer, a_c is the contact area between the needle and the subphase, μ is the subphase viscosity, and L_c' and L_c'' are the characteristic length scales over which the velocity decays in the surface and the subphase, respectively [9]. With no monolayer present, for the same applied force,

$$F = \frac{\mu a_c}{L_c''} v ; \tag{2}$$

v is the needle velocity on the bare subphase. To determine μ_s, we equate Eqs. (1) and (2), assuming that the subphase drag is independent of the monolayer conditions:

$$\frac{\mu a_c}{L_c''} v = \left(\frac{\mu_s P_c}{L_c'} + \frac{\mu a_c}{L_c''}\right) v_1 . \tag{3}$$

From Eq. (3) the Boussinesq number, Bo, which is the ratio of surface drag to subphase drag at these conditions, can be determined [9]:

$$\frac{v}{v_1} - 1 = \frac{\mu_s P_c / L_c'}{\mu a_c / L_c''} = \mathrm{Bo} . \tag{4}$$

When $\mathrm{Bo} \gg 1$, the drag on the probe is primarily from the monolayer; when $\mathrm{Bo} \ll 1$, the drag is primarily from the subphase. If the surface viscosities, $\mu_s(\pi_1)$ and $\mu_s(\pi_2)$,

vary at two different surface pressures (or any other parameters), two different needle velocities, $v_1(\pi_1)$ and $v_2(\pi_2)$ will result from a given F, resulting in Bo (π_1) and Bo (π_2). Taking the ratio of the Bo gives the ratio of the surface viscosity at the different surface pressures, which allows us to determine the viscosity ratio relative to any reference surface viscosity:

$$\frac{\frac{v}{v_2(\pi_2)} - 1}{\frac{v}{v_1(\pi_1)} - 1} = \frac{\mathrm{Bo}(\pi_2)}{\mathrm{Bo}(\pi_1)} = \frac{\mu_s(\pi_2)}{\mu_s(\pi_1)}. \qquad (5)$$

Figure 1 shows $v_1(\pi_1)/v$ (needle speed at constant force normalized to the needle speed at the same force on a subphase with no monolayer) as a function of the monolayer surface pressure for a variety of lipid mixtures that showed a wide range of coexistence between liquid expanded and solid phases. The lipid mixtures were based on human lung surfactant [3,6] and were composed of 77:23 (wt:wt) mixtures of 1,2–dipalmitoyl-*sn*-glycero-3-phosphatidylcholine (DPPC) and 1-palmitoyl-2-oleyl-*sn*-glycero-3-phosphatidylglycerol (POPG) (Avanti Polar Lipids; Alabaster, AL; purity $> 99\%$) with varied amounts of palmitic acid (PA) or *n*-hexadecanol (HD)

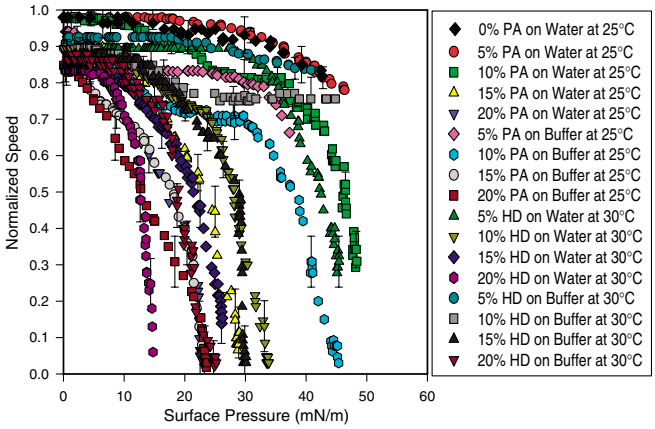

FIG. 1 (color). Speed of magnetic needle on the monolayer of DPPC/POPG with PA or HD as a function of surface pressure, normalized to the speed of the needle at a clean subphase-air interface, v_1/v.

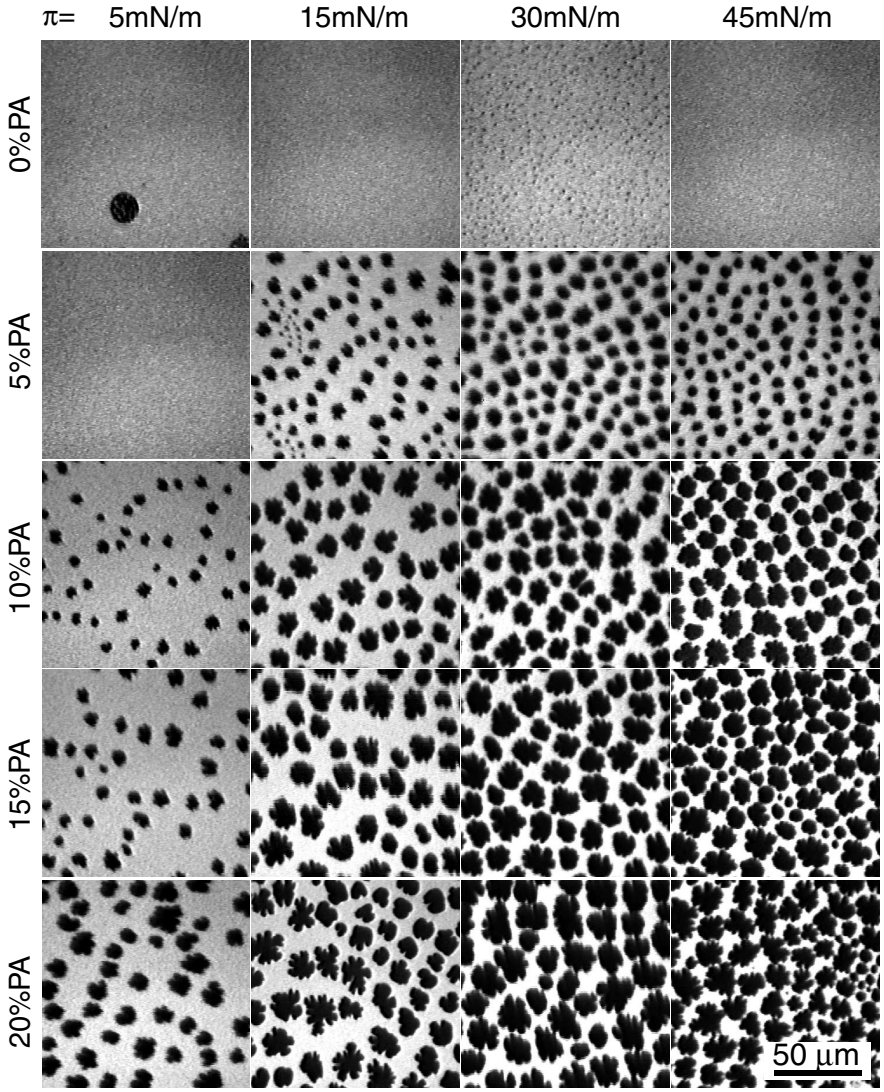

FIG. 2. Fluorescence optical micrographs of monolayers of DPPC/POPG (77:23, wt:wt) with varied amounts of palmitic acid (PA) on a 150 mM NaCl, 5 mM $CaCl_2$, and 0.2 mM $NaHCO_3$ (pH = 6.9) buffer at 25 °C. The PA concentration is labeled in the left of each row, and the top line shows the corresponding surface pressure.

(Sigma Chemical Co. St. Louis, Mo; purity > 99%). Monolayers were spread onto pure water (Millipore Milli-Q system; resistivity > 18 MΩ-cm^{-1}) or a 150 mM NaCl, 5 mM $CaCl_2$, and 0.2 mM $NaHCO_3$ (pH = 6.9) buffer. Figure 1 includes 17 mixtures of DPPC/POPG with PA or HD on water or buffer at 25 °C or 30 °C. We observe two types of behavior. For all mixtures, as the surface pressure increases, the normalized speed decreases. For a few systems such as 5% PA on water or 5% HD on buffer, the normalized needle speed decreases minimally. For the rest of the mixtures, the normalized needle speed gradually decreases with increasing surface pressure, then drops dramatically. For example, in the mixture containing 15% HD on buffer at 30 °C, the needle speed does not change much from 0 to 20 mN/m, but then drops to zero at $\pi \sim 30$ mN/m.

Figure 2 shows the variation of solid/liquid expanded phases in DPPC/POPG/PA monolayers on buffer at 25 °C as a function of surface pressure and PA fraction [13]. The monolayers were prepared from the same lipid mixtures as before but with 0.5 mol% Texas Red DHPE (Molecular Probes, Eugene, OR) added to enable fluorescence imaging. The fluorescent dye partitions preferentially into the liquid-expanded phase, causing it to appear bright and the solid phase dark. To quantify the solid domain fraction, the fluorescence images were digitized and solid domain fraction calculated using a commercial image analysis package (Image-Pro Plus version 4.1, Media Cybernetics, Maryland). Increasing the fraction of PA (or HD, data not shown) increases the fraction of solid phase at a given π and temperature [6,14]. The solid phase is primarily composed of a DPPC/PA (or DPPC/HD) co-crystal [6,14]. POPG is above its critical temperature [15], so the liquid phase is primarily POPG with any DPPC that does not crystallize.

Figure 3 shows the normalized needle speed as a function of solid domain area fraction. For all of the systems examined, the needle speed decreases gradually with solid domain fraction to a solid domain fraction of ~40%. This gradual decrease is followed by a dramatic drop to zero over a narrow range of solid domain fraction between 50% and 60%. The critical area fraction, A_c, is taken to be the solid phase area fraction at which the needle speed goes to zero. The critical area fraction, A_c, depends on the solid domain shapes and polydispersity. Polydisperse circular domains have the highest A_c, more monodisperse, dendritic shaped domains have the lowest A_c. In these experiments, A_c ranged from about 0.5 to about 0.77.

The reduced viscosity, μ_s/μ_{so}, was determined from the normalized needle velocities according to Eq. (5). In three-dimensional dispersions, μ_o is the viscosity of the solvent, or continuous phase, which does not change appreciably with variation in the fraction of solid particles added to the dispersion. Here, μ_{so} was chosen to be the surface viscosity at zero surface pressure and zero solid phase fraction for a given mixture [16]. The normalized needle speed on DPPC/POPG monolayers with no solid phase present

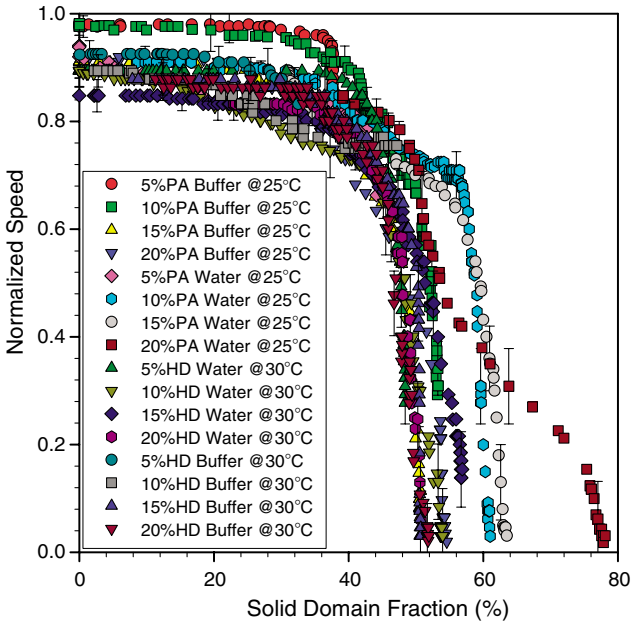

FIG. 3 (color). Speed of magnetic needle, v_1, on monolayers of DPPC/POPG with various amounts of PA or HD as a function of solid domain fraction (determined from fluorescence micrographs, Fig. 2), normalized to the needle speed on the bare subphase, v. The ratio of DPPC/POPG is fixed for all system at 77:23 (wt/wt). The subphase is either pure water or 150 mM NaCl, 5 mM $CaCl_2$, and 0.2 mM $NaHCO_3$ (pH = 6.9) buffer. The critical area fraction, A_c, is taken to be the solid domain fraction at which the normalized speed extrapolates to zero. For the mixtures with a solid phase fraction <0.5, the needle speed only decreases gradually and no A_c was calculated.

shows, within the error of the measurement, that the surface viscosity of the liquid phase does not change significantly up to $\pi \sim 30$ mN/m, so the approximation of constant μ_{so} is not unreasonable.

Figure 4 shows that all of the measured surface viscosity data can be represented as $[1 - (A/A_c)]^{-\beta}$. The surface viscosity effectively diverges at the critical solid area fraction, in direct analogy with three-dimensional suspensions at the close packed volume fraction. Over a wide range of surface pressure, temperature, composition, and domain shape, the surface viscosity of monolayers at a solid-liquid coexistence depends only on the area fraction of solid phase present, in direct analogy to three-dimensional dispersions. The two curves in Fig. 4 show the theoretical limiting curves for strong repulsion, $\mu_s/\mu_{so} = [1 - (A/A_c)]^{-1}$ and for no repulsion, $\mu_s/\mu_{so} = [1 - (A/A_c)]^{-2}$. The exponent of -1 is a surprisingly good fit to the data considering there are no adjustable parameters.

Dougherty and Krieger [17] suggest, based on a different scaling model, that the exponent β should be the product of the intrinsic viscosity, μ_{si} and the critical area fraction, A_c:$\beta = \mu_{si}A_c$. In two-dimensions, $\mu_{si} = \lim_{A\to 0} \frac{[(\mu_s/\mu_{so})-1]}{A}$ and is theoretically predicted to equal 2 [18,19]. According to this model, for our range of A_c (see Fig. 3), β should vary from about 1 to 1.5. However, our data do not suggest a systematic variation

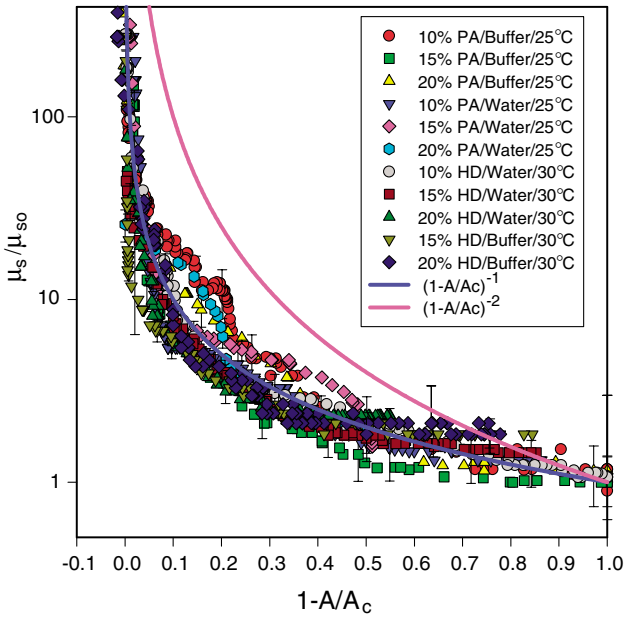

FIG. 4 (color). Semilog plot of (μ_s/μ_{so}) as a function of $(1\text{-}A/A_c)$ derived from the data in Fig. 3 for those mixtures that showed a zero needle velocity so that A_c could be evaluated. The solid curves are the theoretical expressions corresponding to an exponent of -1 (blue) and -2 (red). The excellent fit to the exponent of -1 (no adjustable parameters) shows that there are long-range interactions between the solid domains.

of exponent with A_c, and the Dougherty-Krieger model overestimates the viscosity ratio. In 3D suspensions, it is difficult to distinguish between the Dougherty and Krieger model [17] and the scaling arguments of Brady [7] as they predict similar values for β.

The exponent of -1 suggests that strong repulsive forces exist between the solid particles on a length scale large compared to the hydrodynamic lubrication forces [7]. Both solid and fluid phase domains likely contain charged lipids, PA in the case of the solid domains, and POPG in the case of the fluid domains. Even in uncharged monolayers, different densities and orientations of polar molecules in solid and liquid phases lead to long-range dipole-dipole interactions that can order solid domains over distances large compared to the domain separation [1,2,8]. The surface viscosity is further proof that dipole-dipole interactions are an important determinant of monolayer morphology and mechanics.

The relationship of monolayer composition morphology to physical properties such as surface viscosity is especially important to understanding the function of lung surfactant. Lung surfactant monolayers act to lower the surface tension in order to minimize the work of breathing [20]. A lack of functioning surfactant can lead to respiratory distress syndrome (RDS), a potentially fatal condition in both premature infants and adults [20,21]. On the full compression of the monolayer that results from exhalation, the solid phase fraction of the monolayer could increase past A_c, leading to a rigid monolayer that resists further compression or deformation. These rigid monolayers could be necessary to ensure that the alveoli retain some fraction of residual air volume and do not collapse on exhalation. The high viscosity might also be important during the recruitment of alveoli in the treatment of premature infants with liquid-filled lungs with replacement surfactants. Adjusting the solid phase fraction by composition should lead to the divergence of the surface viscosity of the monolayers occurring at the appropriate part of the breathing cycle.

*To whom correspondence should be directed.
Email address: gorilla@engineering.ucsb.edu

[1] H. McConnell, Ann. Rev. Phys. Chem. **42**, 171 (1991).
[2] H. Mohwald, Ann. Rev. Phys. Chem. **41**, 441 (1990).
[3] J. Ding, D. Takamoto, A. von Nahmen, M. M. Lipp, K. Y. C. Lee, A. J. Waring, and J. A. Zasadzinski, Biophys. J. **80**, 2262 (2001).
[4] B. M. Discher, K. M. Maloney, W. R. Schief, D. W. Grainger, B. Vogel, and S. B. Hall, Biophys. J. **71**, 2583 (1996).
[5] M. M. Lipp, K. Y. C. Lee, D. Y. Takamoto, J. A. Zasadzinski, and A. J. Waring, Phys. Rev. Lett. **81**, 1650 (1998).
[6] F. Bringezu, J. Ding, G. Brezesinski, and J. A. Zasadzinski, Langmuir **17**, 4641 (2001).
[7] J. F. Brady, J. Chem. Phys. **99**, 567 (1993).
[8] M. Seul and D. Andelman, Science **267**, 476 (1995).
[9] C. F. Brooks, G. G. Fuller, C. W. Frank, and C. R. Robertson, Langmuir **15**, 2450 (1999).
[10] J. Ding, H. E. Warriner, and J. A. Zasadzinski, Langmuir **18**, 2800 (2002).
[11] D. K. Schwartz, C. M. Knobler, and A. Bruinsma, Phys. Rev. Lett. **73**, 2841 (1994).
[12] H. A. Stone, Phys. Fluids **7**, 2931 (1995).
[13] M. M. Lipp, K. Y. C. Lee, A. J. Waring, and J. A. Zasadzinski, Rev. Sci. Instrum. **68**, 2574 (1997).
[14] K. Y. C. Lee, J. Majewski, A. von Nahmen, A. Gopal, P. B. Howes, K. Kjaer, G. S. Smith, and J. A. Zasadzinski, J. Chem. Phys. **116**, 774 (2002).
[15] D. Y. Takamoto, M. M. Lipp, A. von Nahmen, K. Y. C. Lee, A. J. Waring, and J. A. Zasadzinski, Biophys. J. **81**, 153 (2001).
[16] For 15% and 20% HD mixtures on buffer, there was a finite solid phase fraction even at zero surface pressure. For these samples, μ_{so} was taken to be the same as the μ_{so} of the 10% HD mixture on buffer that had zero solid phase at zero surface pressure. As primarily HD and DPPC crystallize to form the solid phase, the liquid phase composition in all these mixtures is likely quite similar.
[17] I. M. Krieger, Adv. Colloid. Interface Sci. **3**, 111 (1972).
[18] J. F. Brady, Int. J. Multiphase Flow **10**, 113 (1984).
[19] A. Einstein, Ann. Phys. (Leipzig) **19**, 298 (1906).
[20] J. Goerke, Biochim. Biophys. Acta **1408**, 79 (1998).
[21] J. A. Clements, Physiologist **5**, 11 (1962).